

Text-guided multi-stage cross-perception network for medical image segmentation

gaoyu chen¹ and haixia pan^{1*†}

¹college of software, Beihang University.

*Corresponding author(s). E-mail(s): haixiapan@buaa.edu.cn;

Contributing authors: zy2421102@buaa.edu.cn;

†These authors contributed equally to this work.

Abstract

Medical image segmentation plays a crucial role in clinical medicine, serving as a tool for auxiliary diagnosis, treatment planning, and disease monitoring, thus facilitating physicians in the study and treatment of diseases. However, traditional segmentation methods, such as UNet, are constrained by the weak semantic expression of target regions, which stems from a lack of generalizability and interactivity. To overcome these limitations, incorporating text prompt information holds great potential for accurately pinpointing lesion locations. Despite this, current text-guided methods are hindered by insufficient cross-modal interaction and inadequate cross-modal feature representation. To address these challenges, we propose the Text-guided Multi-stage Cross-perception network (TMC). The TMC incorporates a multi-stage cross-attention module designed to enhance the model’s comprehension of semantic details. Additionally, it introduces a multi-stage alignment loss to improve the consistency of cross-modal semantics. Experimental results demonstrate the superior performance of our TMC, achieving Dice scores of 84.77%, 78.50%, and 88.73% across three public datasets (QaTa-COV19, MosMedData, and Breast), thereby outperforming both UNet-based networks and existing text-guided methods.

Keywords: Vision-Language, Medical image segmentation, Attention mechanism, Cross-perception

1 Introduction

Medical image segmentation is the process of partitioning regions of interest in medical images according to specific requirements, and is a crucial step in medical image processing and analysis[1]. Medical image segmentation aids physicians in accurate diagnosis, treatment planning, and disease monitoring across various clinical applications[2]. Networks such as U-Net[3], UNet++[4] and TransUnet[5] which employ symmetric encoders and decoders along with skip connections, have been widely utilized to perform medical image segmentation tasks. However, these networks often suffer from insufficient feature extraction capabilities and inadequate utilization of contextual information, leading to the inability to effectively learn the discriminative features of lesion areas[6].

Text-guided medical image segmentation, which uses textual annotations to provide specific information to assist image segmentation, can effectively address the limitations of feature extraction and contextual information utilization. For example, LViT[7], which is trained on images and the corresponding text annotations, has significantly enhanced the segmentation performance of medical images. Nevertheless, the insufficient cross-modal interaction between images and text, as well as inadequate cross-modal feature expression result in ineffective utilization of textual information.

To address the issues of insufficient cross-modal interaction and inadequate cross-modal feature expression, this paper proposes the Text-guided Multi-stage Cross-perception network (TMC), which contains two novel modules. Specifically, 1) Multi-stage Cross-attention Module (MCM) drives the model to automatically adjust the attention weights for relevant regions in the image based on the textual description, by enabling dynamic interaction between image features and each word in the text, thereby enhancing the model’s understanding of semantic details. 2) Multi-stage Alignment Loss (MA Loss) facilitates cross-modal alignment of low-level to high-level features between the visual and language encoders, thereby enhancing the consistency of intermediate cross-modal features.

Our contributions are summarized as follows:

- We propose a Text-guided Multi-stage Cross-perception network (TMC) to address the issues of insufficient semantic expression of target regions and inadequate cross-modal interaction.
- The Multi-stage Cross-attention Module (MCM) is proposed to facilitate dynamic interaction between image and text features, thereby effectively capturing the target area in the image by utilizing text prompts.
- The Multi-stage Alignment Loss (MA Loss) is proposed to enhance the consistency between cross-modal features, promoting semantic matching between image and text.
- Extensive experiments are conducted on three publicly available medical image datasets. The comprehensive results demonstrate the effectiveness of each component of the proposed method and show that TMC outperforms existing state-of-the-art methods.

2 Related Works

2.1 Medical Image Segmentation

With the continuous increase in the computational power of devices and the scale of available labeled data, deep learning techniques have developed rapidly and have been widely applied in the field of medical image analysis, especially in medical image segmentation tasks. Long et al. (2015)[8] first proposed the Fully Convolutional Network (FCN) for image segmentation tasks, which replaced fully connected layers with convolutional layers. In the same year, Ronneberger [3] proposed the U-Net model for medical image segmentation, which has become an important baseline model in this field. The U-Net employs a symmetric U-shaped encoder-decoder structure and fuses shallow detail features from the encoder with deep semantic features from the decoder through skip connections. In 2018, Zhou [4] proposed U-Net++ to further improve the segmentation performance of U-Net. TransUNet[5] was an early attempt to integrate Transformers with CNNs for medical image segmentation. However, these methods rely solely on image features to perform segmentation tasks, making it difficult to effectively capture the target segmentation area. In this paper, we leverage text prompt information to improve segmentation performance.

2.2 Text-Guided Medical Image Segmentation

In recent years, the auxiliary semantic information of text has been widely utilized to address the issue of insufficient annotations in the field of medical image segmentation, thereby significantly enhancing segmentation performance.[9] Li et al.[7] proposed the LViT model, which employs a dual-U architecture comprising a U-shaped CNN branch and a U-shaped Vision Transformer (ViT)[10] branch. This model extracts fused image and text features within the U-shaped ViT branch, which are subsequently integrated via a pixel-level attention module (PLAM). The image features enhanced by the text prompts, are ultimately fed into the CNN decoder. Lee et al.[11] introduced the text encoder of CLIP[12], which has been pre-trained on a large-scale language corpus and has demonstrated remarkable performance in various text-related tasks. They utilized this encoder to extract text features and proposed a text-guided cross-position attention module to merge the extracted text features with image features at the bottleneck stage. Compared to segmentation methods that rely solely on image features, these approaches have achieved significant performance improvements, fully demonstrating the great potential of text-guided medical image segmentation. In addition, the ABP[13] introduces an innovative approach that enhances segmentation accuracy by leveraging asymmetric bilateral prompting techniques guided by textual information. The SimTxtSeg[14] proposes a novel framework that leverages simple textual prompts to generate high-quality pseudo-labels for medical image segmentation, featuring a Textual-to-Visual Cue Converter and a Text-Vision Hybrid Attention module to effectively fuse text and image features, achieving state-of-the-art performance on tasks such as colonic polyp and MRI brain tumor segmentation with minimal supervision. However, these methods suffer from insufficient cross-modal interaction and inadequate cross-modal feature expression. These issues may weaken the performance

of information fusion, thereby limiting the guiding role of text semantics in medical image segmentation. In this paper, the Multi-stage Cross-attention Module (MCM) and the Multi-stage Alignment Loss (MA Loss) are proposed to solve these problems.

2.3 Visual Language Model

Visual-language models are designed to integrate visual and linguistic information, with the goal of enabling models to comprehend language descriptions related to visual content or to process visual information based on textual cues. Redford et al. proposed the CLIP[12] model, which employs contrastive learning to automatically identify the associations between images and text. Ji et al. presented the MAP[15] model that leverages self-supervised learning to utilize unlabeled multimodal data for learning a general multimodal representation, which can be applied for multimodal data generation and as a pre-trained model for downstream tasks. Wang et al. proposed the MGCA[16] model to enhance image-text alignment through contrastive learning by constructing a multimodal graph. LoVT[17] is a text-supervised pretraining method for medical image localization tasks, which learns localization representations by contrasting the representations of image regions and report sentences. By integrating instance-level image-report contrastive learning with local contrastive learning, LoVT enhances the model’s ability to understand local features in medical images. GLORIA[18] is a multimodal global-local representation learning framework that learns context-aware representations of medical images by contrasting subregions of medical images with words in paired reports, utilizing both global and local representations simultaneously. PRIOR[19] is a prototypical representation learning framework that combines global and local alignment modules. It enhances the representation learning of medical images and reports by exchanging information between modalities through a cross-modal conditional reconstruction module during the training phase.

3 Method

The TMC proposed in this study is designed for text-guided medical image segmentation and primarily consists of two components. Specifically, Multi-stage Cross-attention Module is designed to drive cross perception between images and text features. Moreover, Multi-stage Alignment Loss performs alignment between images and text at each feature-level to improve the cross-modal consistency.

3.1 Multi-stage Cross-attention Module(MCM)

The Multi-stage Cross-attention Module (MCM) enhances the model’s semantic understanding of target regions by dynamically interacting image features and text features. Our module uses cross-attention mechanisms to automatically adjust the attention weights for relevant regions in the image based on textual descriptions, thereby more accurately localizing target regions. This design not only compensates for the insufficiency of semantic expression in image features but also fully utilizes cross-modal information through multi-stage feature fusion, significantly improving segmentation accuracy.

The Multi-stage Cross-attention Module Fig. 1 designs a multi-stage language encoder and a multi-stage visual encoder. Given an image-text pair, they are respectively fed into the corresponding encoders, with each stage indexed as $i=1,2,\dots,n$. The visual encoder employs the Swin Transformer to capture long-range visual dependencies, and the extracted image features are defined as $V_i \in \mathbb{R}^{H_i W_i \times C_i}$, H_i , W_i , and C_i correspond to the height, width, and channel dimensions of the i^{th} feature, respectively. The language encoder utilizes the BERT-base model, and each encoder extracts language features denoted as $L_i \in \mathbb{R}^{T \times D}$, where T and D represent the text length and feature dimension, respectively. The first token in the language features is the [CLS] token, which contains representative information of all language tokens. The [CLS] token in L_i is defined as $CLS_i \in \mathbb{R}^{1 \times D}$.

The cross-attention module (Fig. 2) integrates visual and language features through the attention mechanism, thereby enriching the contextual information of the visual features. Specifically, the process of vision stage and language stage is described as follows.

$$\begin{aligned} MHCA(Q, K, V) &= Softmax(Q \cdot K^T / \sqrt{d_k}) \cdot V \\ F_V^i &= MLP(MHCA(V_i, L_i)) \\ F_L^i &= MLP(MHCA(L_i, F_V^i)) \end{aligned}$$

where Q , K , V and d_k denote queries, keys, values and dimensions of keys. $MHCA(\cdot)$ and $MLP(\cdot)$ indicate the multi-head cross attention and the Multilayer Perceptron. Through the cross-attention module, the generated visual features F_V^i and language features F_L^i are used as inputs for the next stage.

3.2 Multi-stage Alignment Loss

Our alignment scheme engages the low-level to high-level features in the cross-modal alignment to more effectively embed the intermediate features of the vision and language encoders into the cross-modal embedding space. now we explain the position where the features are aligned for the effective cross-modal fusion and describe how to compute the alignment loss.

The alignment occurs prior to each cross-Attention module, where it aligns the visual and language features. This design enhances the correlation between modalities. The contrastive loss employs the visual feature V_i and the text feature token CLS_i . Both V_i and CLS_i are linearly projected into the same feature dimension D , resulting in the transformed visual feature z_V^i and the transformed text feature z_L^i . The formula for the feature alignment loss is as follows:

$$\begin{aligned} \mathcal{L}_{align}^i &= -\log(\sigma(sim(z_V^i, z_L^i)/\tau_i)) - \log(1 - \sigma(sim(z_V^i, z_L^i)/\tau_i)) \\ \mathcal{L}_{align} &= \frac{1}{n} \sum_{i=1}^n \mathcal{L}_{align}^i \end{aligned}$$

Sim is a cosine similarity, τ is learnable temperature parameters, and σ is a sigmoid function. This loss can effectively address the issue of inadequate cross-modal feature expression.

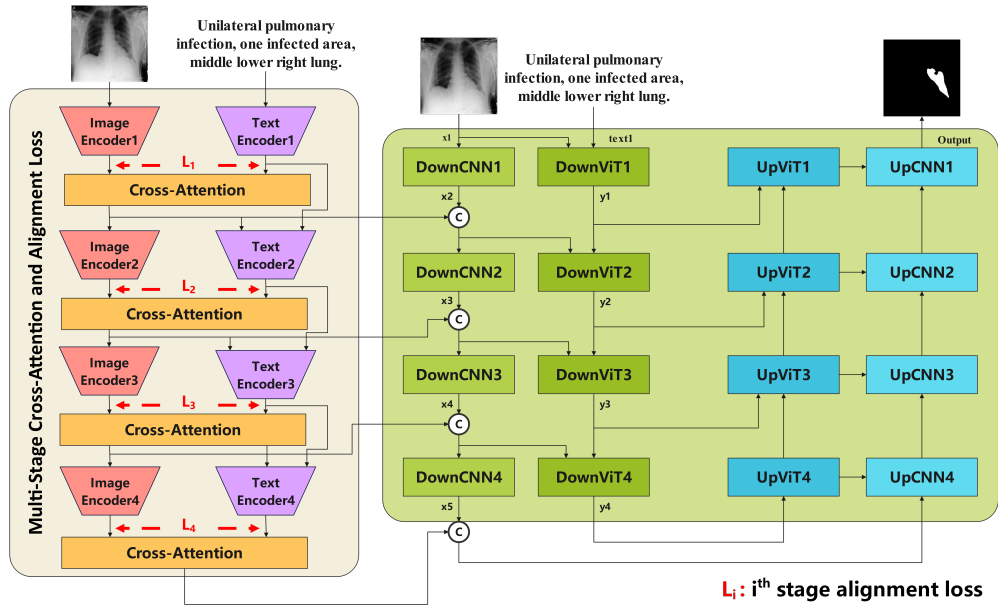


Fig. 1 Text-guided Multi-stage Cross-perception network(TMC)

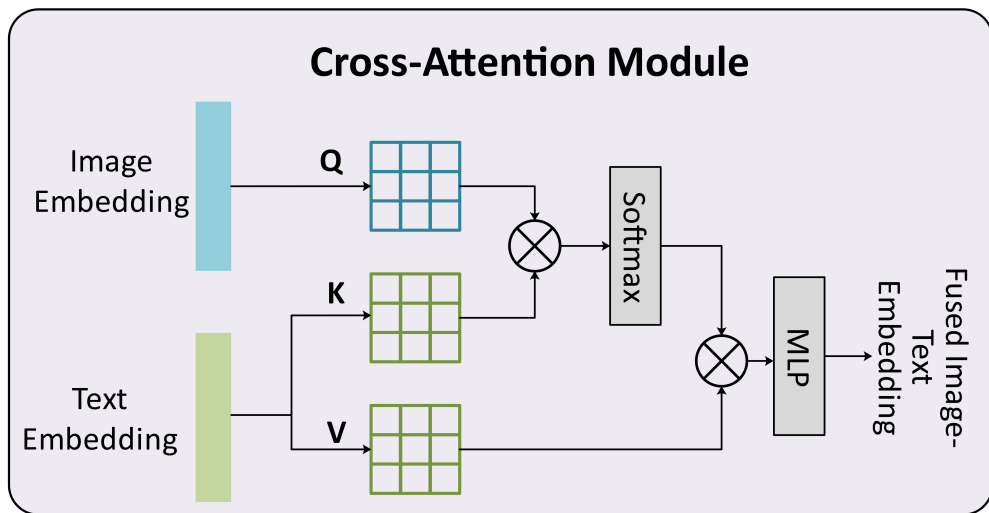


Fig. 2 Cross-Attention Module

3.3 Segmentation Part

We have generated a series of cross-modal features, which need to be effectively integrated into the U-Net model to enhance the model’s feature expression ability and segmentation performance. The process of integration is described as follows.

$$F_i = MCA(V_i, L_i)$$

$$x_i = DownCNN(CONCAT(x_{i-1}, F_i))$$
$$y_i = DownViT(CONCAT(x_{i-1}, F_i), y_{i-1})$$

where x_i and y_i denote the the image features processed by CNN downsampling and the text features processed by ViT downsampling.

3.4 Overall Optimization

The segmentation part is designed with a simple structure. Through the U-shaped architecture, the image is down-sampled and up-sampled via CNN operations, while the text is down-sampled and up-sampled through the ViT module. The visual features processed by the Multi-stage Cross-attention Module are concatenated and fed into the next CNN layer and ViT layer, eventually producing the segmentation output. We use the binary cross-entropy loss \mathcal{L}_{task} for network training. Thus, the final loss function is as follows.

$$\mathcal{L}_{task} = -\frac{1}{N} \sum_{j=1}^N [y_j \log(p_j) + (1 - y_j) \log(1 - p_j)]$$
$$\mathcal{L}_{total} = \mathcal{L}_{task} + \lambda \cdot \mathcal{L}_{align}$$

where N , y_j and p_j denote the total number of the pixels, the truth value and the predicted probability for the j^{th} pixel.

4 Experiment

4.1 Datasets

Extensive experiments were conducted on three publicly available datasets: chest infection area segmentation, nuclei instances segmentation, and breast cancer segmentation.

QaTa-COV19 dataset[20] contains 9258 COVID-19 chest X-ray radiographs. Li et al. [7] provided text annotations and split 7145 samples for training and 2113 samples for testing.

MosMedData dataset[21] containing anonymized chest CT scans with and without COVID-19 related findings. The dataset includes a total of 1,000 CT scans, with 500 normal scans and 500 abnormal scans.

Duke-Breast-Cancer-MRI dataset[22] contains 922 MRI scans from 922 breast cancer patients. The text annotations are provided and verified by two professionals. We divide this dataset into 7:1:2 for training, validation, and testing respectively.

4.2 Implementation Details

Our method is implemented using Pytorch. The operating system is Ubuntu 20.04.4 LTS with 24GB RTX4090 GPU. The learning rate is set to 3e-4 for both the QaTa-COV19 and Duke-Breast-Cancer-MRI datasets, and 1e-3 for the MosMedData dataset. Early stopping is implemented if the model's performance does not improve after 20 epochs based on its current performance. The batch size is 8 for all three dataset.

4.3 Evaluation Metrics

The Dice $Dice = \sum_{i=1}^N \sum_{j=1}^C \frac{1}{NC} \cdot \frac{2|p_{ij} \cap y_{ij}|}{(|p_{ij}| + |y_{ij}|)}$ and mIoU $mIoU = \sum_{i=1}^N \sum_{j=1}^C \frac{1}{NC} \cdot \frac{|p_{ij} \cap y_{ij}|}{|p_{ij} \cup y_{ij}|}$ are used to evaluate our method and other compared methods, where C is the number of categories, and N is the number of pixels.

Method	Text	QaTa-Cov19		MosMedData		Duke-Breast	
		Dice(%)	mIoU (%)	Dice(%)	mIoU (%)	Dice(%)	mIoU (%)
UNet	×	79.94	69.58	74.66	62.54	86.56	79.30
AttUnet	×	77.27	65.95	74.69	62.60	86.53	79.26
nnUNet	×	77.16	65.81	74.52	62.39	85.71	77.99
TransUNet	×	76.98	65.58	74.21	62.00	84.20	75.71
UCTransNet	×	79.26	68.64	77.09	65.72	86.94	79.90
UNet++	×	76.96	65.55	70.13	57.05	86.25	78.82
LViT	✓	83.71	74.98	76.07	64.38	85.55	77.75
CLIP	✓	76.93	65.51	77.59	66.38	86.27	78.86
MAP	✓	74.67	62.58	75.58	63.75	85.92	78.32
MGCA	✓	75.40	63.51	76.43	64.85	85.50	77.67
ours	✓	84.77	76.56	78.50	67.61	88.73	82.74

Table 1 The comparative experiments on the QaTa-COV19, MosMedData and Duke-Breast datasets

Method		QaTa-COV19		MosMedData		Duke-Breast	
MCM	\mathcal{L}_{align}	Dice(%)	mIoU (%)	Dice(%)	mIoU (%)	Dice(%)	mIoU (%)
×	×	83.71	74.98	76.07	64.38	85.55	77.75
✓	×	84.11	75.58	77.27	65.96	87.21	80.32
×	✓	83.96	75.35	77.02	65.63	86.88	79.80
✓	✓	84.77	76.56	78.50	67.61	88.73	82.74

Table 2 Ablation studies demonstrate that significant improvements of the proposed innovations. The results are based on data on the QaTa-COV19, MosMedData and Duke-Breast datasets. MCM: Multi-stage Cross-attention Module; \mathcal{L}_{align} : Multi-stage Alignment loss

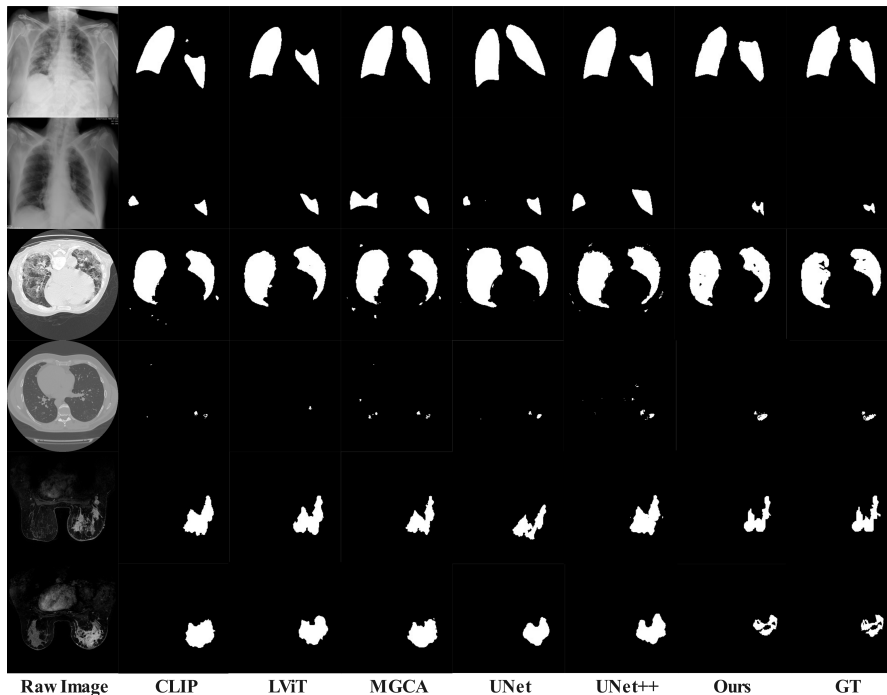


Fig. 3 The visual superiority of the proposed method on QaTa-COV19, MosMedData and Duke-breast datasets. The proposed method shows high-quality segmentation, compared with state-of-the-art methods

4.4 Comparison Study

The TMC is compared with 10 state-of-the-art methods, including U-Net[3], AttUNet[23], nnUNet [24], TransUNet[5], UCTransUNet[25], UNet++[4], LViT[7], CLIP[12], MAP[15] and MGCA[16].

Qualitative Analysis Fig. 3 presents the excellent segmentation performance of our method in comparison with state-of-the-art methods. The proposed method not only accurately locates the target regions but also identifies precise boundaries. As shown in Fig. 3, traditional segmentation methods such as U-Net often misjudge the location of the target regions, while vision language methods like LViT and CLIP inaccurately determine the boundaries. These issues arise due to insufficient cross-modal interaction and inadequate cross-modal feature expression.

Quantitative Analysis Our TMC achieves highly competitive performance on three datasets against existing state-of-the-art methods. Table 1 indicates that our TMC outperforms all the other methods in both Dice (84.77%) and mIoU (76.56%) from the QaTa-Cov19 dataset. It is evident that the proposed method outperforms the aforementioned traditional segmentation methods and visual-language methods, thereby demonstrating the model’s capability to accurately locate target regions through text guidance. Table 1 also demonstrates the superiority of our method on the MosMedData and Duke-Breast datasets. Overall, our TMC achieves the best

results across different segmentation tasks, thereby proving the method’s excellent generalization and robustness.

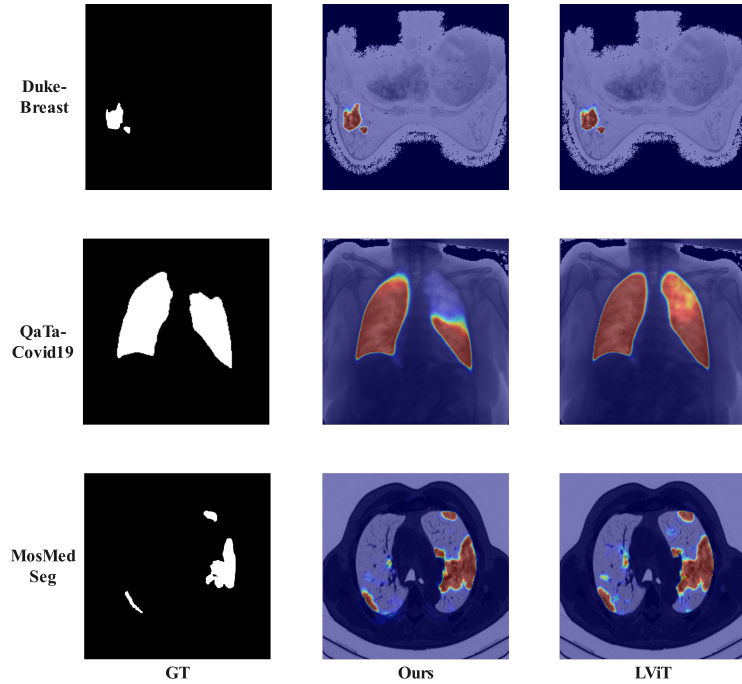


Fig. 4 The heatmap demonstrates the strong capability of our TMC in capturing the lesion regions.

4.5 Ablation Study

We perform ablation experiments to verify the contribution of novel designs, and the number of segmentation model parameters does not increase after adding novel designs.

Effectiveness of MCM. Table 2 shows that removing the MCM limits the performance, resulting in a decrease of 0.81% in Dice and 1.21% in mIoU on the QaTa-Cov19 dataset. This indicates that MCM addresses the issue of insufficient cross-modal interaction through cross-modal attention.

Effectiveness of MA loss Table 2 shows that removing the MA loss limits the performance, resulting in a decrease of 0.66% in Dice and 0.98% in mIoU on the QaTa-Cov19 dataset. This indicates that MA loss addresses the issue of inadequate cross-modal feature expression by calculating the loss across modalities.

4.6 Interpretability Analysis

The figure 4 shows the different heatmap on the different dataset. The figure shows that the TMC model demonstrates higher precision in the segmentation of lesion areas.

Compared to other models, the TMC model can more accurately locate the lesion regions. It also shows better clarity in identifying the boundaries of these regions, indicating that the model can more finely capture the edges of the lesions. These advantages give the TMC model a significant edge in medical image segmentation tasks.

5 Conclusion

In this paper, we propose a novel text-guided medical image segmentation model called TMC, which addresses the issues of insufficient cross-modal interaction and inadequate cross-modal feature expression through multi-stage cross-modal attention and multi-stage cross-modal alignment loss. It enhances the model’s semantic understanding of target regions by automatically adjusting the attention weights for relevant regions in the image based on textual descriptions, thereby more accurately localizing target regions. Experimental results demonstrate that our TMC outperforms SOTA methods.

Declarations

The authors declare that no funds, grants, or other support were received during the preparation of this manuscript. The authors declare that no funds, grants, or other support were received during the preparation of this manuscript.

References

- [1] Withey, D.J., Koles, Z.J.: A review of medical image segmentation: methods and available software. *International Journal of Bioelectromagnetism* **10**(3), 125–148 (2008)
- [2] Dai, L., Johar, M.G.M., Alkawaz, M.H.: Review of semi-supervised medical image segmentation based on the u-net. *Academic Journal of Science and Technology* (2024)
- [3] Ronneberger, O., Fischer, P., Brox, T.: U-net: Convolutional networks for biomedical image segmentation. In: *Medical Image Computing and Computer-assisted intervention—MICCAI 2015: 18th International Conference, Munich, Germany, October 5-9, 2015, Proceedings, Part III* 18, pp. 234–241 (2015). Springer
- [4] Zhou, Z., Rahman Siddiquee, M.M., Tajbakhsh, N., Liang, J.: Unet++: A nested u-net architecture for medical image segmentation. In: *Deep Learning in Medical Image Analysis and Multimodal Learning for Clinical Decision Support: 4th International Workshop, DLMIA 2018, and 8th International Workshop, ML-CDS 2018, Held in Conjunction with MICCAI 2018, Granada, Spain, September 20, 2018, Proceedings 4*, pp. 3–11 (2018). Springer

- [5] Chen, J., Lu, Y., Yu, Q., Luo, X., Adeli, E., Wang, Y., Lu, L., Yuille, A.L., Zhou, Y.: Transunet: Transformers make strong encoders for medical image segmentation. arXiv preprint arXiv:2102.04306 (2021)
- [6] Milletari, F., Navab, N., Ahmadi, S.-A.: V-net: Fully convolutional neural networks for volumetric medical image segmentation. In: 2016 Fourth International Conference on 3D Vision (3DV), pp. 565–571 (2016). Ieee
- [7] Li, Z., Li, Y., Li, Q., Wang, P., Guo, D., Lu, L., Jin, D., Zhang, Y., Hong, Q.: Lvit: language meets vision transformer in medical image segmentation. IEEE transactions on medical imaging **43**(1), 96–107 (2023)
- [8] Long, J., Shelhamer, E., Darrell, T.: Fully convolutional networks for semantic segmentation. In: Proceedings of the IEEE Conference on Computer Vision and Pattern Recognition, pp. 3431–3440 (2015)
- [9] Ryu, J.S., Kang, H., Chu, Y., Yang, S.: Vision-language foundation models for medical imaging: a review of current practices and innovations. Biomedical Engineering Letters, 1–22 (2025)
- [10] Dosovitskiy, A., Beyer, L., Kolesnikov, A., Weissenborn, D., Zhai, X., Unterthiner, T., Dehghani, M., Minderer, M., Heigold, G., Gelly, S., et al.: An image is worth 16x16 words: Transformers for image recognition at scale. arXiv preprint arXiv:2010.11929 (2020)
- [11] Lee, G.-E., Kim, S.H., Cho, J., Choi, S.T., Choi, S.-I.: Text-guided cross-position attention for segmentation: Case of medical image. In: International Conference on Medical Image Computing and Computer-Assisted Intervention, pp. 537–546 (2023). Springer
- [12] Radford, A., Kim, J.W., Hallacy, C., Ramesh, A., Goh, G., Agarwal, S., Sastry, G., Askell, A., Mishkin, P., Clark, J., et al.: Learning transferable visual models from natural language supervision. In: International Conference on Machine Learning, pp. 8748–8763 (2021). PmLR
- [13] Zeng, X., Zeng, P., Cui, J., Li, A., Liu, B., Wang, C., Wang, Y.: Abp: Asymmetric bilateral prompting for text-guided medical image segmentation. In: International Conference on Medical Image Computing and Computer-Assisted Intervention, pp. 54–64 (2024). Springer
- [14] Xie, Y., Zhou, T., Zhou, Y., Chen, G.: Simtxtseg: Weakly-supervised medical image segmentation with simple text cues. In: International Conference on Medical Image Computing and Computer-Assisted Intervention, pp. 634–644 (2024). Springer
- [15] Ji, Y., Wang, J., Gong, Y., Zhang, L., Zhu, Y., Wang, H., Zhang, J., Sakai, T., Yang, Y.: Map: Multimodal uncertainty-aware vision-language pre-training

- model. In: Proceedings of the IEEE/CVF Conference on Computer Vision and Pattern Recognition, pp. 23262–23271 (2023)
- [16] Wang, F., Zhou, Y., Wang, S., Vardhanabhuti, V., Yu, L.: Multi-granularity cross-modal alignment for generalized medical visual representation learning. *Advances in Neural Information Processing Systems* **35**, 33536–33549 (2022)
- [17] Zhang, Y., Jiang, H., Miura, Y., Manning, C.D., Langlotz, C.P.: Contrastive learning of medical visual representations from paired images and text. In: *Machine Learning for Healthcare Conference*, pp. 2–25 (2022). PMLR
- [18] Huang, S.-C., Shen, L., Lungren, M.P., Yeung, S.: Gloria: A multimodal global-local representation learning framework for label-efficient medical image recognition. In: *Proceedings of the IEEE/CVF International Conference on Computer Vision*, pp. 3942–3951 (2021)
- [19] Müller, P., Kaissis, G., Zou, C., Rueckert, D.: Joint learning of localized representations from medical images and reports. In: *European Conference on Computer Vision*, pp. 685–701 (2022). Springer
- [20] Degerli, A., Kiranyaz, S., Chowdhury, M.E., Gabbouj, M.: Osegnet: Operational segmentation network for covid-19 detection using chest x-ray images. In: *2022 IEEE International Conference on Image Processing (ICIP)*, pp. 2306–2310 (2022). IEEE
- [21] Morozov, S.P., Andreychenko, A.E., Pavlov, N.A., Vladzimirskyy, A., Ledikhova, N.V., Gombolevskiy, V.A., Blokhin, I.A., Gelezhe, P.B., Gonchar, A., Chernina, V.Y.: Mosmeddata: Chest ct scans with covid-19 related findings dataset. *arXiv preprint arXiv:2005.06465* (2020)
- [22] Saha, A., Harowicz, M.R., Grimm, L.J., Kim, C.E., Ghate, S.V., Walsh, R., Mazurowski, M.A.: A machine learning approach to radiogenomics of breast cancer: a study of 922 subjects and 529 dce-mri features. *British journal of cancer* **119**(4), 508–516 (2018)
- [23] Oktay, O., Schlemper, J., Folgoc, L.L., Lee, M., Heinrich, M., Misawa, K., Mori, K., McDonagh, S., Hammerla, N.Y., Kainz, B., et al.: Attention u-net: Learning where to look for the pancreas. *arXiv preprint arXiv:1804.03999* (2018)
- [24] Isensee, F., Jaeger, P.F., Kohl, S.A., Petersen, J., Maier-Hein, K.H.: nnu-net: a self-configuring method for deep learning-based biomedical image segmentation. *Nature methods* **18**(2), 203–211 (2021)
- [25] Wang, H., Cao, P., Wang, J., Zaiane, O.R.: Uctransnet: rethinking the skip connections in u-net from a channel-wise perspective with transformer. In: *Proceedings of the AAAI Conference on Artificial Intelligence*, vol. 36, pp. 2441–2449 (2022)